

Improved Data Reduction for Far-Infrared/Submillimeter Polarimetry

LARRY KIRBY,¹ JACQUELINE A. DAVIDSON,² JESSIE L. DOTSON,³ C. DARREN DOWELL,⁴ AND ROGER H. HILDEBRAND^{1,5}

Received 2005 April 20; accepted 2005 June 17; published 2005 August 19

ABSTRACT. Fluctuations in atmospheric emission introduce noise and systematic errors into measurements of polarization at far-infrared and submillimeter wavelengths. We describe a new analysis method that corrects for the bias and reduces the errors caused by the fluctuations. The method exploits repeated observations of a source and is especially effective on faint sources for which the polarized flux is on the same order as the atmospheric fluctuations.

1. INTRODUCTION

We have re-examined the techniques of data reduction used in far-infrared and submillimeter polarimetry in which measurements are limited by atmospheric fluctuations. Both the transmitted flux from the source and the emitted flux from the atmosphere are affected by these fluctuations. The transmission effects at these wavelengths can be effectively removed by measuring orthogonal components of polarization simultaneously (Hildebrand et al. 1984, 2000), as has been done with polarimeters such as Hertz (Schlenning et al. 1997; Dowell et al. 1998), Stokes (Platt et al. 1991), and SPARO (Submillimeter Polarimeter for Antarctic Remote Observations; Renbarger et al. 2004). The fluctuations in emission are largely removed by rapid optical switching, or “chopping,” between on-source and off-source positions. Linear gradients in the emission are removed by moving the telescope, “nodding,” to sample off-source positions on both sides of the source. But since atmospheric emission varies in position and time, there is always a residual sky noise that is not removed by chopping and nodding (Li et al. 2005). Some submillimeter cameras use off-source edge pixels to determine the residual sky noise (Greaves et al. 2003). However, this method is flawed for extended sources larger than the detector array.

The residual sky noise has not prevented extensive measurements of polarization of bright objects (Dotson et al. 2000). However, for fainter objects, the residual sky noise may be as large as the flux from the source, preventing any significant measurements.

Here we describe a method to reduce the effects of residual sky noise and related systematic errors (Li et al. 2005) by averaging flux measurements after correcting for the optical depth and air mass.

2. OLD METHOD

It will simplify the discussion to review the data-reduction method that has been previously used. The radiation entering the polarimeter passes through a half-wave plate and is then split into orthogonal components by a grid of parallel wires. The components reflected and transmitted by the grid are detected simultaneously by separate arrays of detectors. The differences and sums of the corresponding signals are recorded as the half-wave plate is stepped from one position, θ , to the next. In the previous method, the reflected and transmitted components R and T of polarization were combined in the following manner:

$$S(\theta) = \frac{R(\theta) - fT(\theta)}{R(\theta) + fT(\theta)}, \quad (1)$$

where f is a gain factor between the two arrays used to correct for differences in sensitivity between the detectors, and $S(\theta)$ is the “polarization signal.” A series of measurements such that the phase of the signal varies through 2π is called a “file.” For a single position of the detector array on the sky, files are repeated a few times for bright sources, and many times for faint sources. As θ is varied, the polarization signal varies sinusoidally. The degree and angle of polarization are derived from the amplitude and phase, taking into account sky rotation and the projection of the wire grid onto the sky. The derivation begins with a determination of reduced Stokes parameters q and u , where q is the ratio of the difference in amplitude between orthogonal components measured in a particular coordinate system (e.g., north-south and east-west) to the total flux from the source, while u is the ratio of the difference in amplitude between the components with respect to a coordinate system rotated 45° from the first one to the total flux (e.g.,

¹ Enrico Fermi Institute and Department of Astronomy and Astrophysics, University of Chicago, 5640 South Ellis Avenue, Chicago, IL 60637; lkirby@oddjob.uchicago.edu, roger@oddjob.uchicago.edu.

² SOFIA-USRA, NASA/Ames Research Center, Moffett Field, CA 94035; j davidson@sofia.usra.edu.

³ NASA/Ames Research Center, Moffett Field, CA 94035; dotson@mail.arc.nasa.gov.

⁴ California Institute of Technology, Jet Propulsion Laboratory, Pasadena, CA 91109; cdd@submm.caltech.edu.

⁵ Department of Physics, University of Chicago.

Hildebrand et al. 2000). The q and u from all of the files are then put through a multiple linear regression that returns q_s , q_t , q_i , u_s , u_t , and u_i , which are the reduced Stokes parameters from the source, telescope, and instrument, respectively (Platt et al. 1991). The degree P and position angle ϕ of the polarization are related to the reduced Stokes parameters by

$$P^2 = q^2 + u^2 \quad (2)$$

$$\phi = \frac{1}{2} \arctan\left(\frac{u}{q}\right). \quad (3)$$

The beauty of this method is that changes in absorption affect the R and T arrays equally and therefore do not affect the ratio in equation (1). This method has been very successful at detecting polarization of bright sources like the Orion molecular cloud (Schleuning 1998) and the Galactic center (Dowell et al. 1998; Novak et al. 2000). There has been less success with faint sources, however. While the effects of atmospheric absorption have been removed, the effects of residual sky noise have not. The residual sky noise is assumed to be unpolarized and therefore is split equally into the two arrays and is removed in the numerator of equation (1), but not removed in the denominator. Therefore, $S(\theta)$ from equation (1) is the polarized flux from the source, divided by the sum of the sky-attenuated flux from the source and the residual sky noise s :

$$S(\theta) = \frac{a(t)PF_0 \sin(4\theta)}{a(t)F_0 + s}, \quad (4)$$

where $a(t)$ is the sky transmission at time t , and F_0 is the unattenuated flux from the source. Bright sources are affected only by a slight increase in the noise, as the residual sky noise is much smaller than the flux from the source. For fainter sources the residual sky noise can be as large as the flux from the source, causing a bias that washes out the polarization signal.

In the limit that the residual sky noise is completely removed from the numerator, the residual sky noise in the denominator still introduces a bias in $S(\theta)$. The expectation value of $S(\theta)$ is therefore proportional to the expectation value of F_{obs}^{-1} , where $F_{\text{obs}} = R(\theta) + fT(\theta) = a(t)F_0 + s$. Assuming a residual sky noise that is Gaussian and an F_{obs} having mean μ and variance σ , this bias can be computed. Figure 1 shows a plot of this bias versus μ/σ , which is the signal-to-noise ratio. At values of μ/σ less than ~ 1.3 , individual measurements of F_{obs} are frequently negative, switching the sign of the polarization signal. Switching the sign is equivalent to shifting the phase of $S(\theta)$ by 180° . Averaging the out-of-phase signals results in a lower polarization. At values of μ/σ greater than ~ 1.3 , F_{obs} is rarely negative; however, there will be a positive bias, because $\langle F_{\text{obs}}^{-1} \rangle$ is less than $\langle F_{\text{obs}}^{-1} \rangle$ for a symmetric distribution. There is an additional positive bias (not shown in Fig. 1) that results from combining q and u in quadrature (Rice 1947; Wardle & Kronberg 1974; Simmons & Stewart 1985). However, this bias

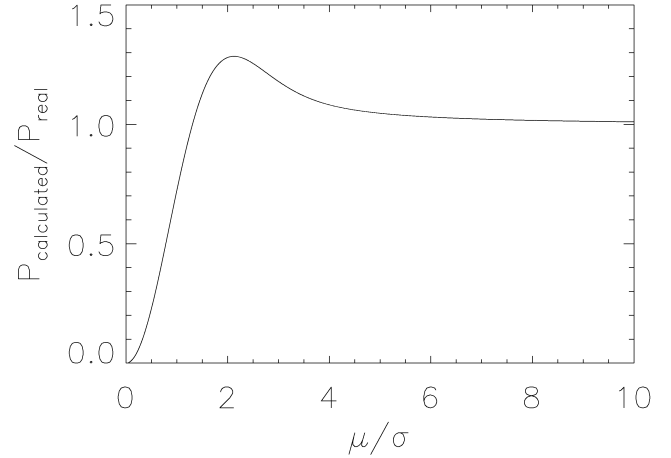


FIG. 1.—Bias (old method) on the measured polarization due to residual sky noise in F_{obs} vs. the signal-to-noise (μ/σ). Plot is generated by computing the expectation value of $\mu/(R + fT)$. The bias in the figure is not the total bias, but only that from the calculation of F_{obs} .

is small ($\leq 10\%$) for points $\geq 3\sigma$ (e.g., see § 4.2 of Hildebrand et al. 2000).

3. NEW METHOD

As before, the two arrays are combined into F_{obs} and $(R - fT)$, but q and u are not derived after each file. Here F_{obs} is related to F_0 by

$$F_{\text{obs}} = a(t)F_0 + s. \quad (5)$$

After several files, one can expect $\langle s \rangle \rightarrow 0$ and

$$\frac{\langle F_{\text{obs}} \rangle}{\langle a(t) \rangle} \rightarrow F_0. \quad (6)$$

Since F_0 is constant, it can be determined by averaging over a series of measurements, such as the F_{obs} for all θ for all of the files taken in a night or series of nights. The error on F_{obs} is taken to be the standard deviation between all values of F_{obs} in the file. The error on F_0 comes from propagating the error on F_{obs} .

The transmission along the line of sight at time t is given by

$$a(t) = e^{-\tau(t)AM(t)}, \quad (7)$$

where τ is the optical depth (transmission at the zenith is given by $e^{-\tau}$) and $AM = \text{air mass} = \text{secant of the zenith angle}$. The optical depth is measured periodically—typically at 225 GHz and at 10 minute intervals—by a “sky dip” instrument at the observatory, and the measured value is corrected to the wavelength of the polarization measurement. To find the best value of $\tau(t)$ at the time of a given file, one fits a polynomial to the

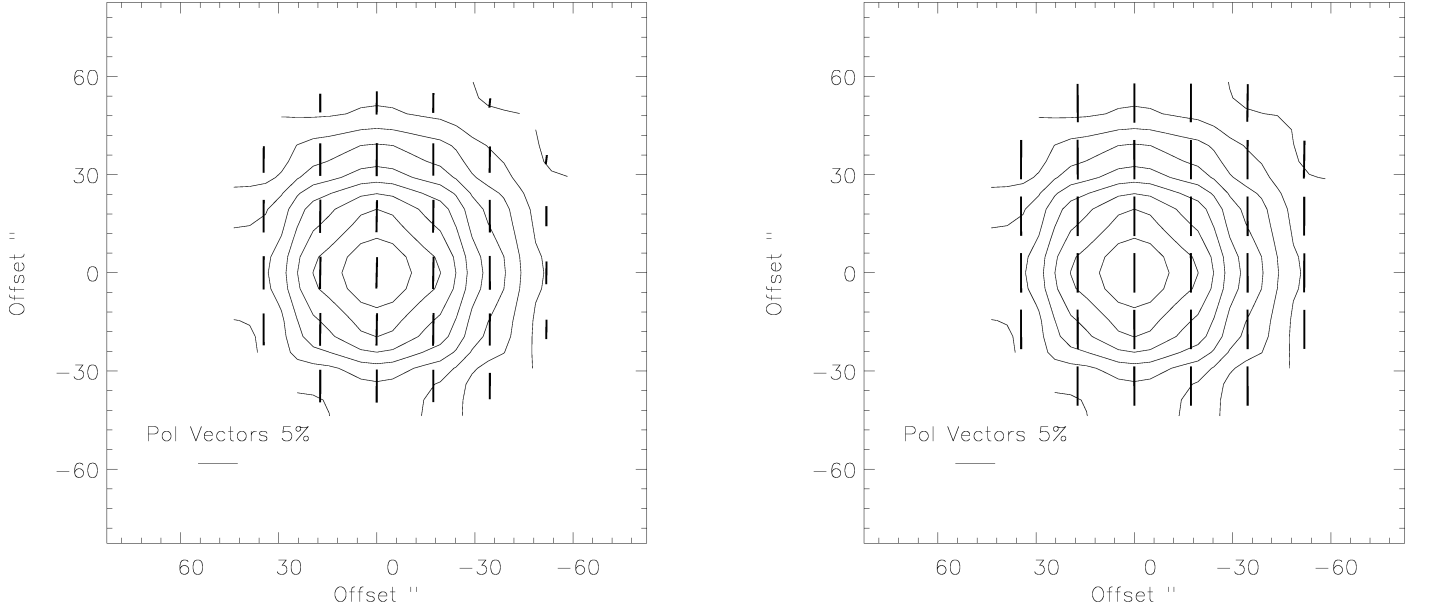


FIG. 2.—Plot of simulated observations with $F_0/\sigma_{\text{rsn}} = 10$, using both the old method (*left*) and the new method (*right*) for a source of intensity $I \propto e^{0.2r^2}$, where r is distance from the center in pixels. Source has 5% polarization in the north-south direction. Contours come from F_0 as computed in eq. (6). Vector lengths are scaled by degree of polarization.

data from the individual sky dips to smooth and interpolate between the measurements (Archibald et al. 2002).

From the sinusoidal variations of the term $(R - fT)$, one obtains observed values Q_{obs} and U_{obs} of the signals for the (nonreduced) Stokes parameters, where $Q_{\text{obs}} = a(t)Q_0$ and $U_{\text{obs}} = a(t)U_0$. From these, one obtains the reduced Stokes parameters

$$q = \frac{Q_{\text{obs}}}{a(t)F_0}, \quad (8)$$

$$u = \frac{U_{\text{obs}}}{a(t)F_0}. \quad (9)$$

The uncertainties in q and u are combinations of the uncertainties from the fitting of Q and U and that from F_0 . The q and u from each file are then used in the multiple linear regression as in the old method.

4. COMPARISON OF OLD AND NEW METHODS

To compare the two methods, observations of a source with a Gaussian random residual sky noise were simulated. The residual sky noise was sampled from a Gaussian centered on zero, and the source flux was set to be either 10 times or equal to the standard deviation of the residual sky noise, σ_{rsn} . The observed intensity was set to be the sum of the attenuated emission from the source and the residual sky noise term. The residual sky noise term is randomized for every frame (see

Hildebrand et al. 2000 for Hertz observing protocol) and was the same across the entire array. The τ was set to be a random number between 1.00 and 1.50 (typical values at Mauna Kea at $350 \mu\text{m}$). The polarization was set at 5% and in the northerly direction for all positions. Figure 2 shows the result when the source flux is 10 times larger than the σ_{rsn} . The two maps are practically indistinguishable, except at the lowest contours, where the new method shows improvement. The old method therefore works well for bright sources where F_0/s is large.

Figure 3 shows the result when the source flux is equal to σ_{rsn} . Here there is a clear difference between the two methods. In the old method, a number of points (*circles*) have 2σ upper limits $\leq 1\%$ polarization, and the points that have $\geq 3\sigma$ detections (*vectors*) have values that are less than the actual 5% of the source. The new method correctly accounts for the residual sky noise; therefore, the plot from this method looks similar to that from Figure 2.

Figure 4 shows data from Houde et al. (2004) of OMC-3 MMS 6, analyzed using both methods, displaying the improvement with the new method on an actual source. In the new method, there are 23 additional detections of $\geq 3\sigma$.

5. SUMMARY

Simultaneous measurements of orthogonal components of polarization effectively remove the effect of atmospheric fluctuations on the transmission of radiation from the source of interest, but only partially remove the effect of fluctuations in atmospheric emission. This problem is especially serious for

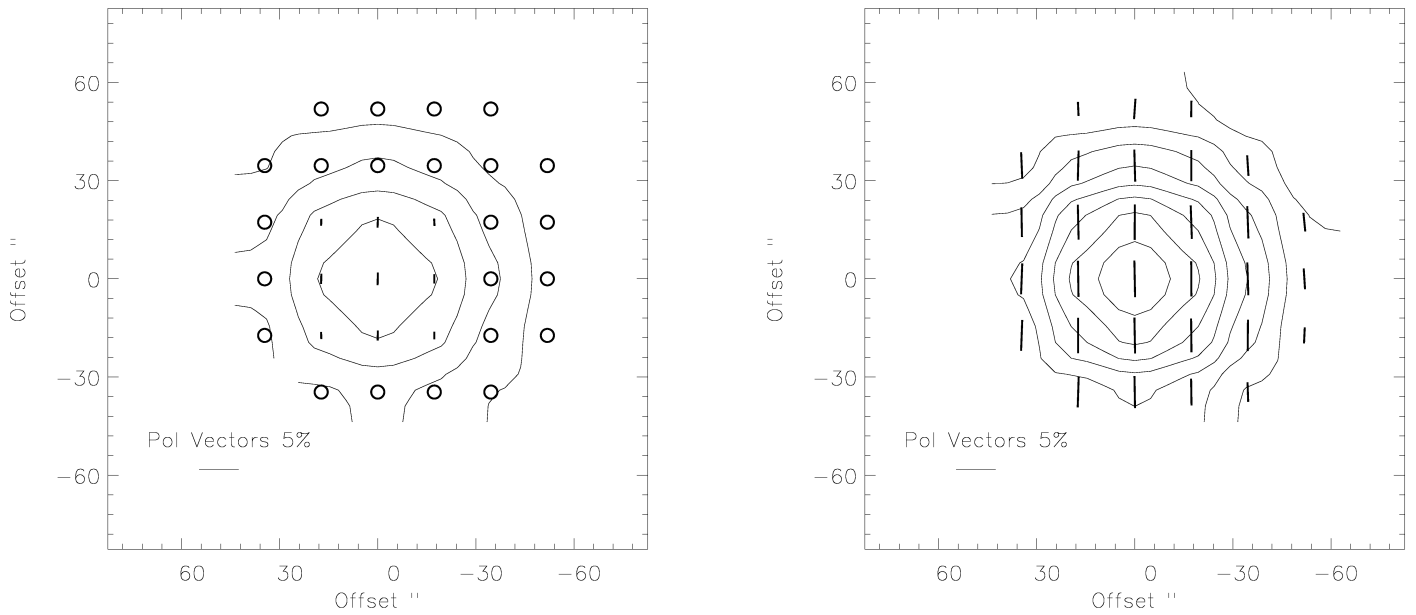


FIG. 3.—Plot of simulated observations with $F_0/\sigma_{\text{rsn}} = 1$, using both the old method (*left*) and the new method (*right*) for the same intensity profile as Fig. 2. Source has 5% polarization in the north-south direction. Contours come from F_0 as computed in eq. (6). Vector lengths are scaled by degree of polarization. Circles indicate points with a 2σ upper limit of 1%.

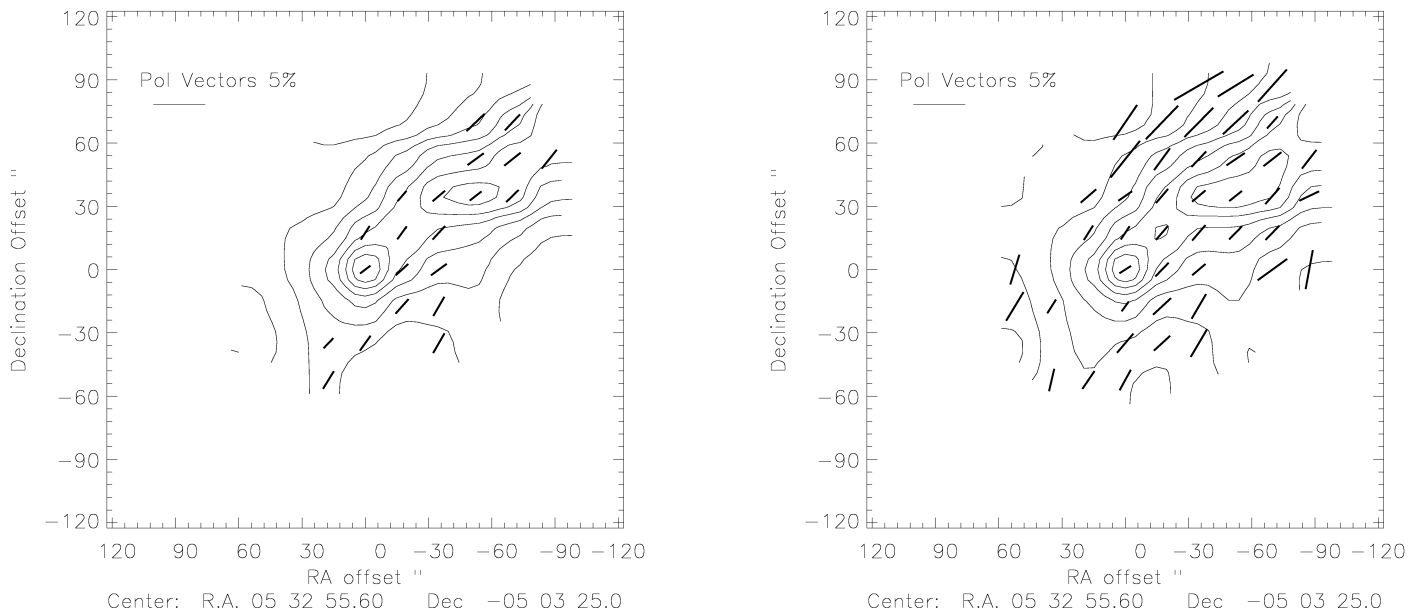


FIG. 4.—Plots of OMC-3 MMS 6 analyzed with the old method (*left*) and the new method (*right*). Contours come from F_0 as computed in eq. (6). Vector lengths are scaled by degree of polarization. Coordinates are B1950.0.

faint sources in which the polarized flux may be smaller than the fluctuations in sky emission. We have described a method of analysis that significantly reduces the errors due to this effect. To apply the method, one must have repeated observations of the source and measurements of the atmospheric optical depth.

We would like to thank Hua-Bai Li, John Vaillancourt, Ler-othodi Leeuw, Giles Novak, Dave Chuss, Martin Houde, and Michael Attard for their comments and suggestions. This work was supported by NSF grant AST 02-04886.

REFERENCES

- Archibald, E. N., et al. 2002, *MNRAS*, 336, 1
 Dotson, J. L., Davidson, J. A., Dowell, C. D., Schleuning, D. A., & Hildebrand, R. H. 2000, *ApJS*, 128, 335
 Dowell, C. D., Hildebrand, R. H., Schleuning, D. A., Dotson, J. L., Novak, G., Renbarger, T., & Houde, M. 1998, *ApJ*, 504, 588
 Greaves, J. S., et al. 2003, *MNRAS*, 340, 353
 Hildebrand, R. H., Davidson, J. A., Dotson, J. L., Dowell, C. D., Novak, G., & Vaillancourt, J. E. 2000, *PASP*, 112, 1215
 Hildebrand, R. H., Dragovan, M., & Novak, G. 1984, *ApJ*, 284, L51
 Houde, M., Dowell, C. D., Hildebrand, R. H., Dotson, J. L., Vaillancourt, J. E., Phillips, T. G., Peng, R., & Bastien, P., 2004, *ApJ*, 604, 717
 Li, H., Griffin, G. S., Krejny, M., Novak, G., Lowenstein, R. F., Newcomb, M. G., Calisse, P. G., & Chuss, D. T. 2005, in *ASP Conf. Ser. Astronomical Polarimetry, Current Status and Future Directions* (San Francisco: ASP), in press
 Novak, G., Dotson, J. L., Dowell, C. D., Hildebrand, R. H., Renbarger, T., & Schleuning, D. A. 2000, *ApJ*, 529, 241
 Platt, S. R., Hildebrand, R. H., Pernic, R., Davidson, J. A., & Novak, G. 1991, *PASP*, 103, 1193
 Renbarger, T., et al. 2004, *PASP*, 116, 415
 Rice, S. O. 1947, *Bell System Tech. J.*, 27, 109
 Schleuning, D. A. 1998, *ApJ*, 493, 811
 Schleuning, D. A., Dowell, C. D., Hildebrand, R. H., & Platt, S. R. 1997, *PASP*, 109, 307
 Simmons, J. F. L., & Stewart, B. G., 1985, *A&A*, 142, 100
 Wardle, J. F. C., & Kronberg, P. P., 1974, *ApJ*, 194, 249